

## HEAT-TRANSFER ANALYSIS OF SUPERCRITICAL-WATER- AND SUPERHEATED-STEAM-COOLED CHANNELS OF SCWR

**Eu. Saltanov, W. Peiman, Sh. Draper and I. Pioro**

Faculty of Energy Systems and Nuclear Science  
University of Ontario Institute of Technology (UOIT)  
2000 Simcoe Str. North, Oshawa, Ontario, L1H 7K4 Canada

[eugene.saltanov@hotmail.com](mailto:eugene.saltanov@hotmail.com), [wargha.peiman@gmail.com](mailto:wargha.peiman@gmail.com), [shona\\_faye@hotmail.com](mailto:shona_faye@hotmail.com),  
[igor.pioro@uoit.ca](mailto:igor.pioro@uoit.ca)

### Abstract

SuperCritical-Water-cooled Reactors (SCWRs) are being developed as one of the Generation-IV nuclear-reactor concepts. Main objectives of the development are to increase thermal efficiency of a Nuclear Power Plant (NPP) and to decrease capital and operational costs. The first objective can be achieved by introducing nuclear steam-reheat inside a reactor and utilizing regenerative feedwater heaters. The second objective can be achieved by designing a steam cycle that closely matches that of the mature supercritical fossil-fuelled power plants.

A detailed steam-cycle layout of a 1200-MW<sub>el</sub> SCWR, which was scaled from a single-reheat 660-MW<sub>el</sub> modern thermal-power plant is presented in the paper. Heat transfer calculations were made for SuperCritical-Water (SCW) and SuperHeated-Steam (SHS) channels of the proposed reactor concept. In the calculations a uniform and three non-uniform Axial Heat Flux Profiles (AHFPs) were considered for two different fuels (UO<sub>2</sub> and MOX). Bulk-fluid, sheath, and fuel centerline temperatures as well as Heat Transfer Coefficient (HTC) profiles were obtained along fuel channels. The HTC values are within a range of 4.7 – 20 kW/(m<sup>2</sup>·K) and 9.7 – 10 kW/(m<sup>2</sup>·K) for the SCW and SHS channels respectively.

**Keywords:** Steam Cycle, Supercritical Water, Heat Transfer Calculations

### 1. Introduction

Since the 80's, the advancements in metallurgical technology have significantly improved the reliability of SuperCritical (SC) steam turbines. As a result, SC turbines have been widely deployed in newly built fossil-fuelled power plants. The gross overall steam-cycle efficiency of SC power plants reached typically 47% – 54%, corresponding to 38% – 43% in net plant efficiency (on a Higher-Heating Value (HHV) basis).

An analysis of SC-turbine data [1] showed that:

- The vast majority of the modern and upcoming SC turbines are single-reheat-cycle turbines;

- Major “steam” inlet parameters of these turbines are: The main or primary SC “steam” –  $P = 24 - 25$  MPa and  $T = 540 - 600^{\circ}\text{C}$ ; and the reheat or secondary subcritical-pressure steam –  $P = 3 - 5$  MPa and  $T = 540 - 620^{\circ}\text{C}$ .
- Usually, the main “steam” and reheat-steam temperatures are the same or very close (for example,  $566/566^{\circ}\text{C}$ ;  $579/579^{\circ}\text{C}$ ;  $600/600^{\circ}\text{C}$ ;  $566/593^{\circ}\text{C}$ ;  $600/620^{\circ}\text{C}$ ).
- Only very few double-reheat-cycle turbines were manufactured so far. The market demand for double-reheat turbines disappeared due to economic reasons after the first few units were built.

Therefore, currently supercritical turbines used in fossil-fueled plants are designed for reheat-steam cycles. Besides cycle efficiency improvement, steam-reheat implementation reduces the steam flow required for a given power output, and furthermore, it reduces the steam moisture content in the LP turbine, thus eliminating the need for moisture-removal equipment. 25 MPa and  $600^{\circ}\text{C}$  are common steam parameters in state-of-the-art fossil-fueled power plants. Therefore, it is reasonable to develop steam cycle for SCW NPP similar to that of fossil-fueled plants, so that conventional SC turbines can be used. Fig. 1 represents a detailed thermal layout of a modern thermal-power plant with steam superheating section operating in Tom'-Usinsk, Russia. The original layout for  $660\text{ MW}_{\text{el}}$  was scaled to  $1200\text{ MW}_{\text{el}}$ .

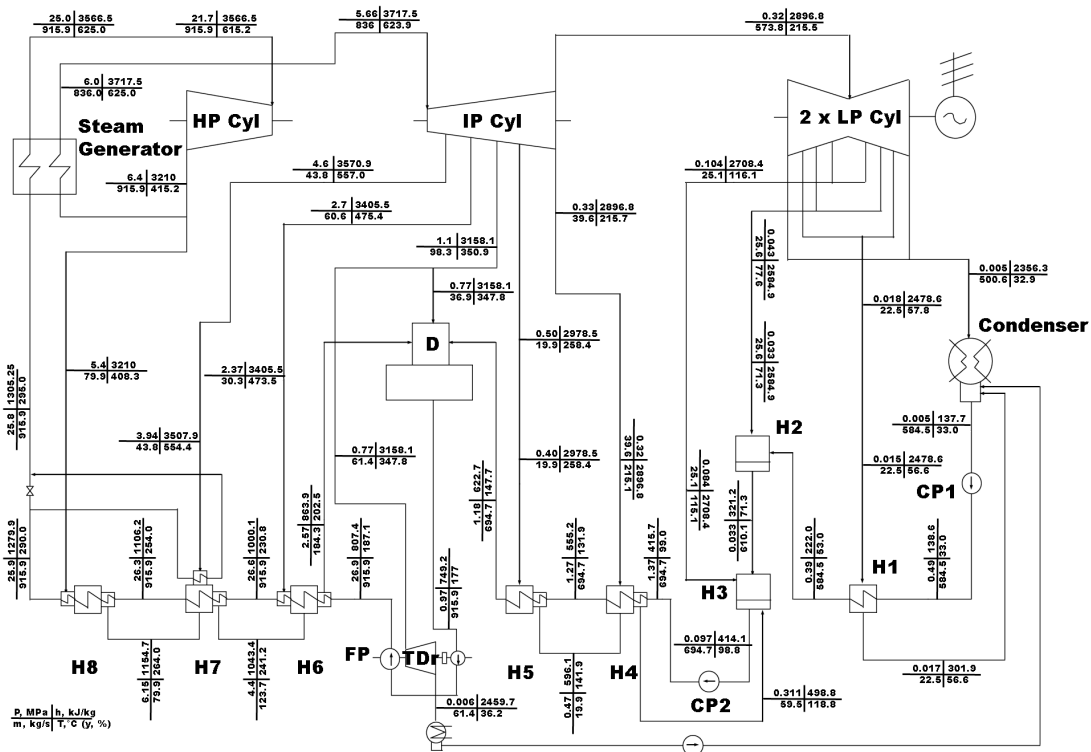
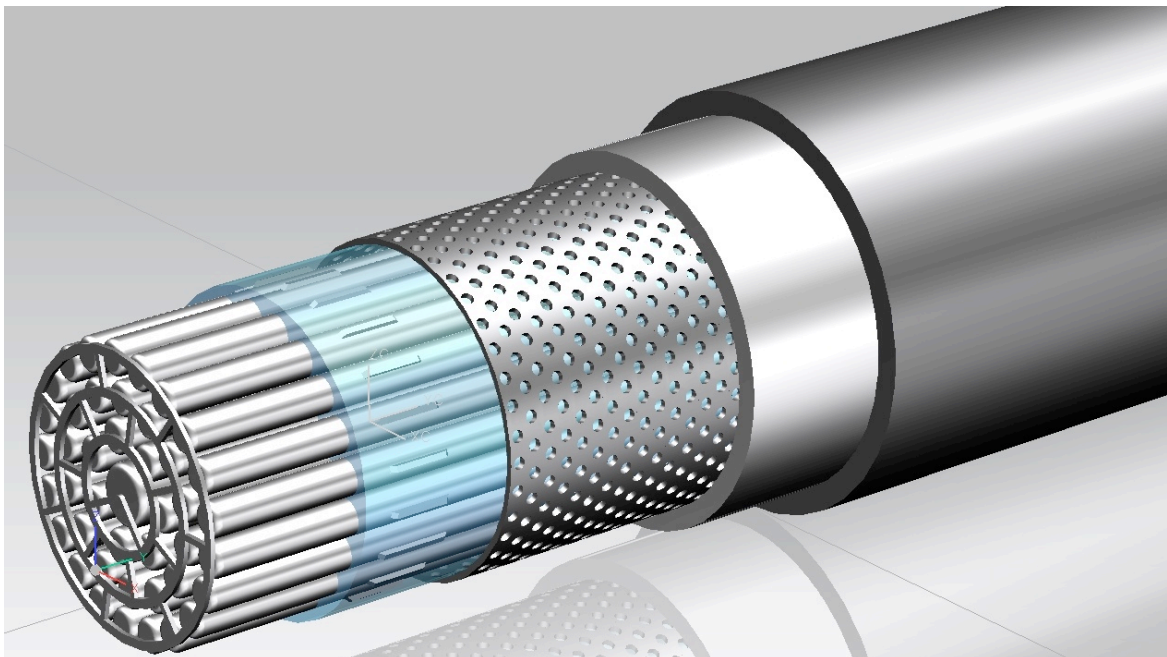


Figure 1. Scaled thermal layout of single-reheat-cycle  $660\text{-MW}_{\text{el}}$  Tom'-Usinsk thermal power plant (Russia) thermal layout to  $1200\text{-MW}_{\text{el}}$  variant (Kruglikov et al., 2009): Cyl – Cylinder; H – Heat exchanger (feedwater heater); FP - Feedwater pump; CP – Condenser Pump; and TDr – Turbine Drive;

Recalculation was made based on mass flow and heat balance. Pressure drop along line was recalculated in proportion to the square of the ratio of the recalculated mass-flow rate to the reference mass-flow rate. This is valid assuming that differences in densities at the recalculated and reference temperatures are negligible. Rebalancing feedwater heaters and condenser required iterative search, since for these elements both mass and energy were to be conserved. Coolant at the deaerator and condenser outlets was assumed to be at saturated state.

## 2. Heat-transfer calculations for SCW and SHS channels

It is envisaged that a generic SCWR will consist of 220 SCW channels and 80 SHS channels. SHS channels are placed in the periphery of the core. SCW at a temperature of about 350°C will enter the core and heated there up to temperature of about 625°C. The HP turbine inlet pressure will be about 25 MPa. After expansion to the SHS state ( $P \approx 6.1\text{MPa}$ ,  $T \approx 350 - 400^\circ\text{C}$ ) it will be sent back to the reactor and superheated there to temperature of about 625°C and then sent to the IP section of the turbine [1]. Currently, the conceptual SHS channel doesn't differ from SCW channel, since the upper limits for operating temperatures are assumed the same - 625°C. The ceramic-insulated fuel channel consists of a liner tube, ceramic insulator, and pressure tube, as shown in Fig. 2. The main purpose of the liner tube, which is a perforated tube, is to protect the ceramic insulator during re-fuelling and operation with fuel bundles inside. The ceramic insulator, which is 70% porous and made of Yttria-Stabilized Zirconia (YSZ), should provide good thermal insulation [2].



**Figure 2. 3-D View of Ceramic-Insulated Fuel Channel for SCWRs [2].**

As mentioned above, water at supercritical state will be used in the generic SCWR. All thermophysical parameters experience significant change near the pseudocritical point.

Variations of certain thermophysical properties of water along SCW channel are plotted in the Fig. 3 and 4 (values of the properties were calculated using NIST (2007) software). The values of volumetric expansivity, Prandtl number, and specific heat experience 8 – 10 fold increase in the vicinity of the pseudocritical point. The values of viscosity, thermal conductivity and density drop 4 – 5 times in the vicinity of the pseudocritical point.

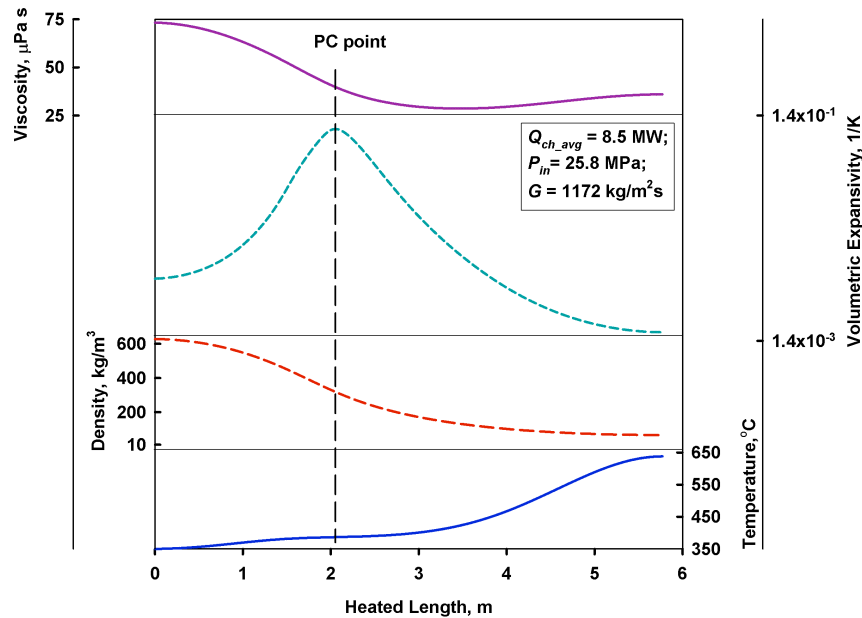


Figure 3. Variation of density, viscosity, and volumetric expansivity of water along SCW channel.

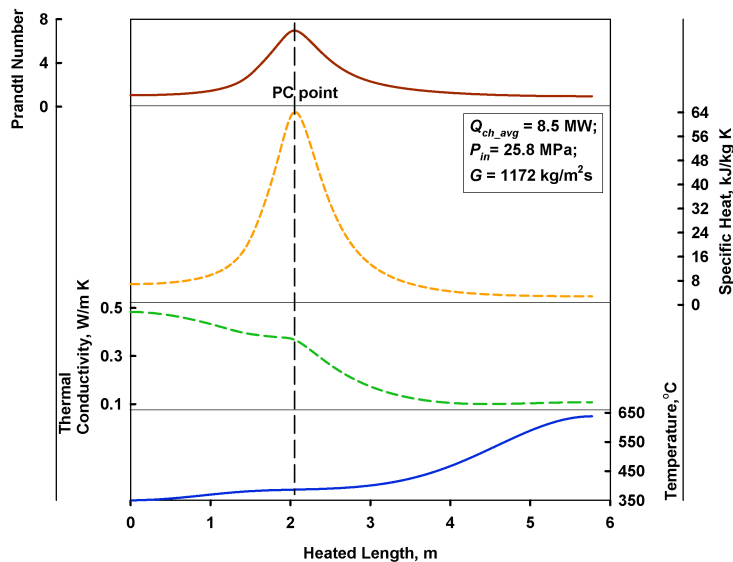


Figure 4. Variation of thermal conductivity, Prandtl number, and specific heat of water along SCW channel.

Heat-transfer calculations were made for a channel with Variant-20 bundles (central unheated rod, 42 heated rods of equal diameter). The mathematical model consists of two parts: (a) calculation of the hydraulic-equivalent diameter,  $D_{hy}$ , for the given geometry of the channel, and (b) calculation of bulk-fluid, fuel-element sheath, and fuel centerline temperatures along the channel.

In the part (a), the values of PT inner diameter,  $D_{PT,i}$ , outer diameter of the fuel-element sheath,  $D_{SH,o}$ , outer diameter of the central unheated control rod,  $D_{UH}$ , and number of fuel elements,  $N_{SH}$ , are the input parameters. Then area blocked by fuel elements, flow area, wetted perimeter, and  $D_{hy}$  are calculated (Equations 1 – 4):

$$A_{block} = \frac{\pi}{4} (N_{SH} D_{SH,o}^2 + D_{UH}^2) \quad (1)$$

$$A_{fl} = \frac{\pi}{4} D_{PT,i}^2 - A_{block} \quad (2)$$

$$p_{wet} = \pi (D_{PT,i} + N_{SH} D_{SH,o} + D_{UH}) \quad (3)$$

$$D_{hy} = \frac{4 A_{fl}}{p_{wet}} = \frac{D_{PT,i}^2 - (N_{SH} D_{SH,o}^2 + D_{UH}^2)}{D_{PT,i} + N_{SH} D_{SH,o} + D_{UH}} \quad (4)$$

The calculated value of  $D_{hy} = 7.83$  mm for Variant-20 bundle.

In the part (b), first of all, the linear flux shape was set up. Four Axial Heat-Flux Profiles were considered: uniform, truncated cosine, upstream-skewed, and downstream-skewed. The truncated cosine and upstream-skewed profiles were taken as proposed in [3]. Downstream-skewed profile was obtained by symmetrical reflection of upstream-skewed profile with respect to longitudinal center of the channel. This idea was proposed in [4]. The AHFPs are plotted in Fig. 5.

After this the inlet values of temperature and inlet and outlet value of pressure are input. Linear pressure drop along the channel was assumed. Then iterative loop for calculation of temperatures distribution was implemented. Channel length was sliced into elementary pieces, each 1 mm long. For piece  $i$ , value of specific enthalpy  $h_i$  was retrieved from NIST, specific enthalpy at the end of the piece,  $h_{i+1}$  was calculated from the heat balance on the piece, and  $T_{i+1}$  was retrieved from NIST:

$$h_i = f(T_i, P_i); \quad \dot{m}(h_{i+1} - h_i) = \dot{q}'_{i+1} \Rightarrow h_{i+1} = \frac{\dot{q}'_{i+1}}{\dot{m}} + h_i; \quad T_{i+1} = f(h_{i+1}, P_{i+1}) \Rightarrow h_{i+2} = f(T_{i+1}, P_{i+1}) \text{ and so on}$$

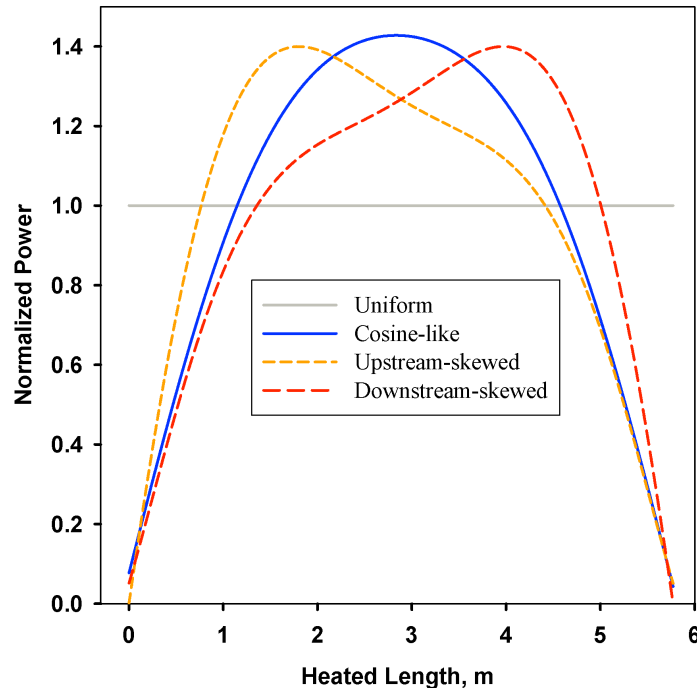


Figure 5. Various AHFPs used for heat-transfer calculations (based on [3]).

In a recent research on creating look-up tables for trans-critical heat transfer [5] it was shown that the best agreement with the data in the supercritical water and superheated steam region had the correlation developed by Mokry et al. [6]. Therefore, in the model, Mokry et al. correlation was used to determine HTC for both SCW and SHS:

$$\text{Nu}_b = 0.0061 \text{Re}_b^{0.904} \overline{\text{Pr}}_b^{0.684} \left( \frac{\rho_w}{\rho_b} \right)^{0.564}, \quad (5)$$

where dimensionless groups were calculated from their definitions as follows:

$$\text{Nu}_b = \frac{h_{tc} \cdot D_{hy}}{k}; \quad \text{Re}_b = \frac{4\dot{m}}{\mu \cdot \pi D_{hy}}; \quad \overline{\text{Pr}}_b = \frac{\mu}{k} \cdot \underbrace{\frac{h_w - h_b}{T_w - T_b}}_{c_p} \quad (6)$$

Mokry et al. correlation requires iteration be made to calculate  $T_w$ . Therefore, for the first piece of channel initial guess of  $T_w$  was made, HTC was calculated from Mokry et al. correlation, and corrected value of  $T_{w,1}$  was calculated from Newton's cooling law. The iterations for the piece were stopped after difference of wall temperatures  $T_w$  and  $T_{w,1}$  became less than 0.1 K. For all the next pieces the initial guess of wall temperature was equal to:  $T_{w,i+1} = T_{b,i+1} + (T_{w,i} - T_{b,i})$ . This approach saved about 35,000 iteration for the channel. HTC profiles along SCW and SHS channels are plotted in Fig. 6.

After determining wall temperature, inner sheath temperature was determined from Fourier's law, assuming that the sheath material is Inconel-718. Its thermal conductivity depends on temperature, according to [7], as:

$$k = 11.45 + 1.156 \cdot 10^{-2} T + 7.72 \cdot 10^{-6} T^2, \quad (6)$$

where  $T$  is measured in °C.

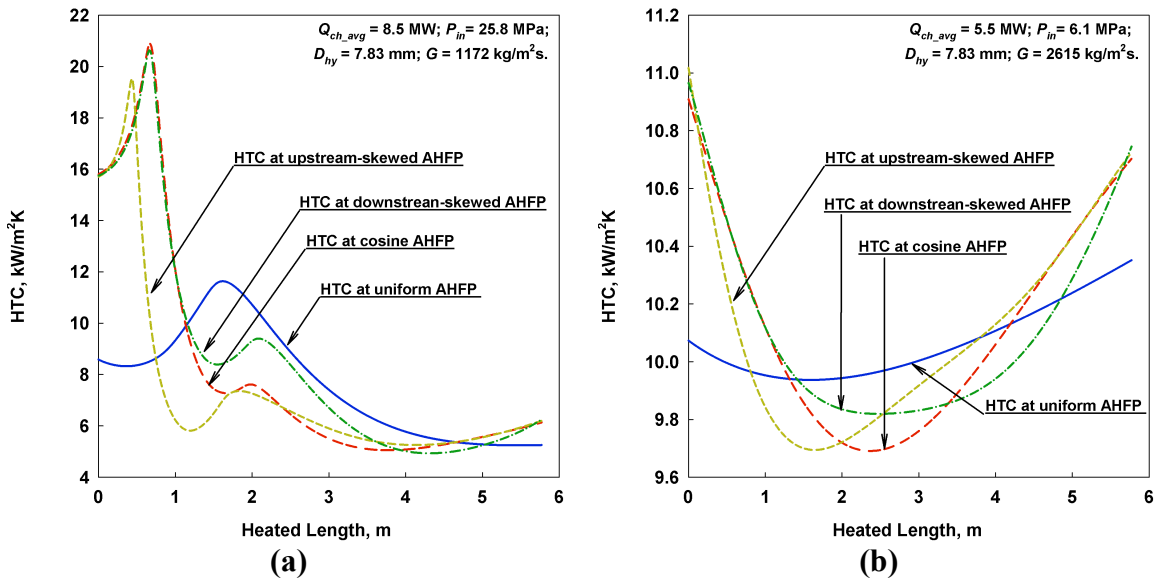


Figure 6. AHFPs profiles along SCW (a) and SHS (b) at average channel power

Fuel centerline temperature was calculated by calculating by dividing fuel pellet radius into  $10^4$  elements and calculating temperature increase across each successive ring towards the center. Different fuels were considered as the alternative to  $UO_2$  due to its possible inadmissible high temperature in a SCW channel. Figures 7-10 represent bulk-fluid, fuel-element sheath, and fuel centerline temperature distributions along SCW and SHS channels at uniform and downstream-skewed AHFPs for  $UO_2$  and MOX.

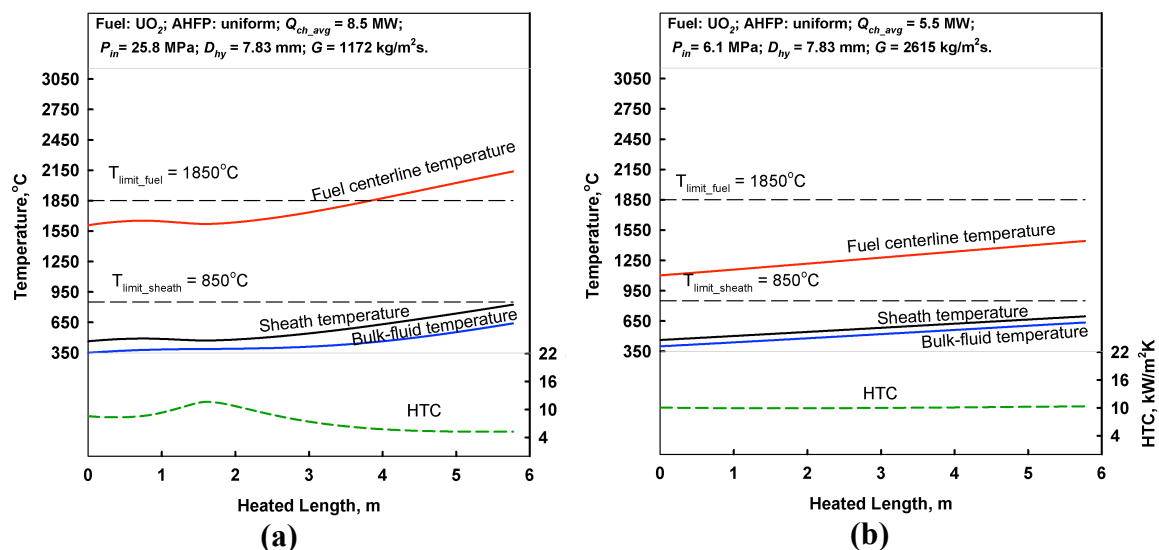
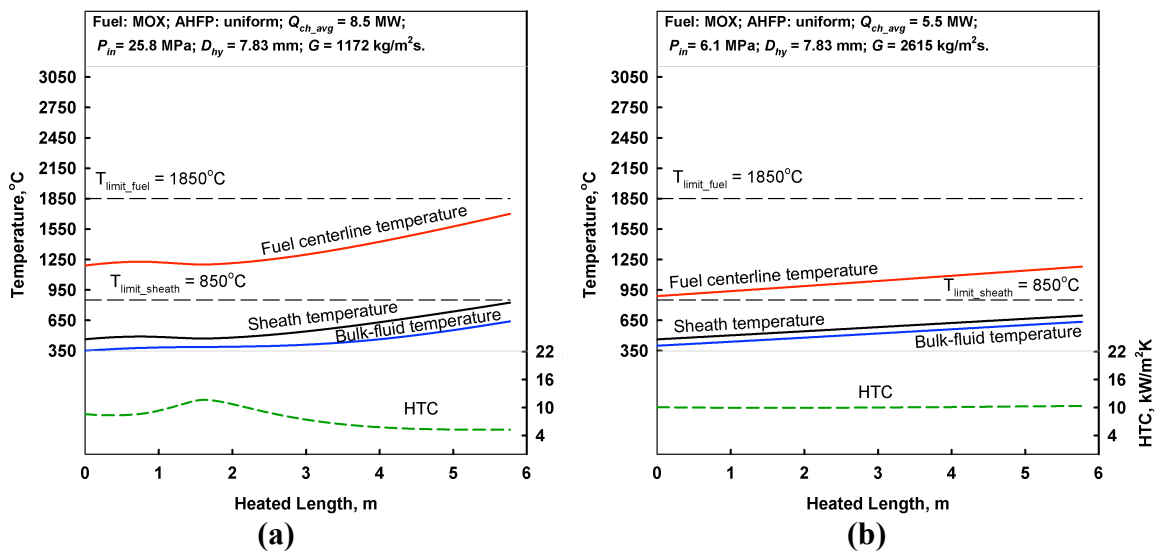
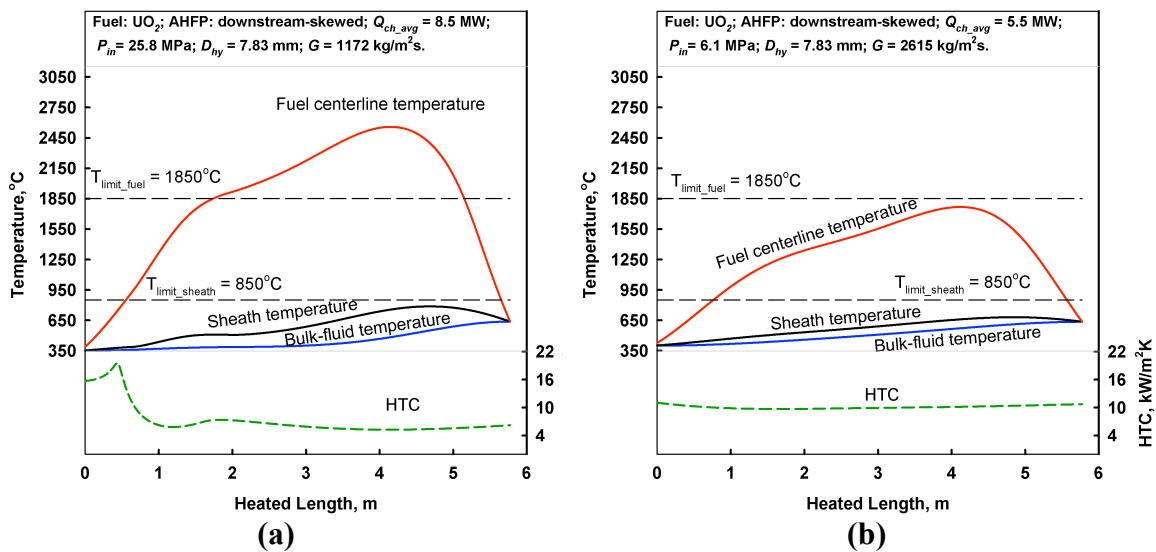


Figure 7. Temperature profiles at average power, uniform AHFP.

(a) – SCW, (b) – SHS channel. Fuel:  $UO_2$ .



**Figure 8. Temperature profiles at average power, uniform AHFP.**  
**(a) – SCW, (b) – SHS channel. Fuel: MOX.**



**Figure 9. Temperature profiles at average power, downstream-skewed AHFP.**  
**(a) – SCW, (b) – SHS channel. Fuel: UO<sub>2</sub>.**

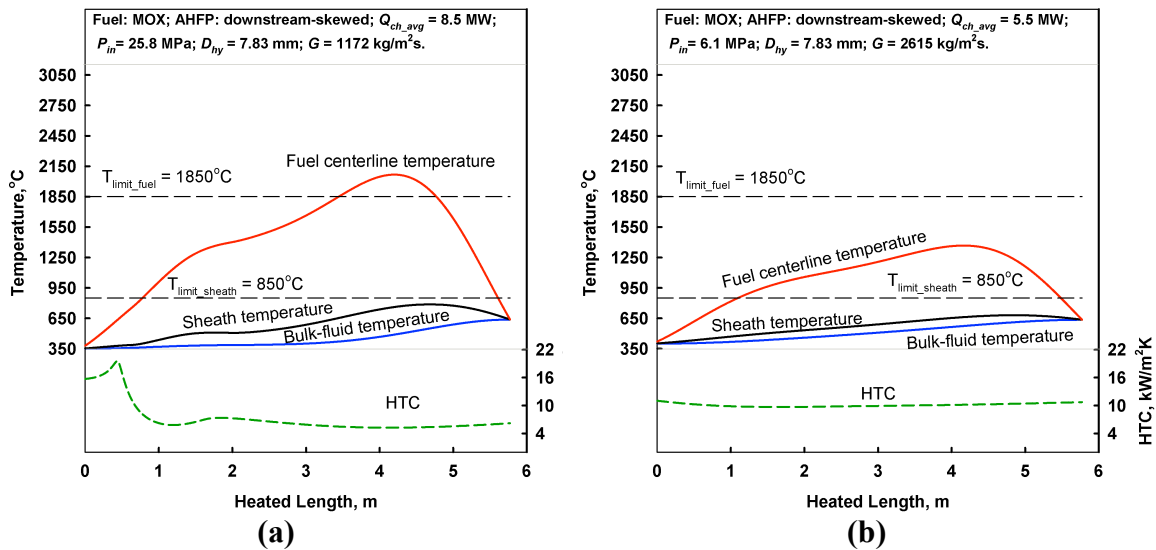


**Figure 10. Temperature profiles at average power, downstream-skewed AHFP. (a) – SCW, (b) – SHS channel. Fuel: MOX.**

It may be seen from the graphs, that there is an accelerated rise in the temperatures closer to the outlet of the channel at downstream-skewed AHFP. In all cases the highest temperature is reached at the downstream-skewed AHFP, the least stresses temperature conditions are achieved at upstream-skewed AHFP. Calculations showed that centerline temperature would exceed design limit for UO<sub>2</sub> and MOX fuels when used in a SCW channel. We estimate that centerline temperature will stay 600°C below the limit for fuels with significantly higher thermal conductivity than that of UO<sub>2</sub>, for example, UC<sub>2</sub>, or UN. For a SHS channel conditions, centerline temperatures of both fuels stay below the design limit. The peak values of fuel centerline temperatures at different AHFPs in SCW and SHS channel are presented in Table 1.

**Table 1. Peak values of fuel (b) centerline temperatures (°C) in SCW and SHS channels at average power.**

AHFP/Fuel	UO <sub>2</sub>		MOX	
	SCW	SHS	SCW	SHS
Uniform	2139 <sup>1</sup>	1429	1701	1180
Cosine	2559	1393	2068	1245
Upstream-skewed	2361	1382	1779	1431
Downstream-skewed	2615	1419	2098	1389

<sup>1</sup> Temperature values in red are those exceeding industry accepted limit for UO<sub>2</sub> of 1850°C

As it may noted from the table, centerline temperature temperatures drops by at least approximately 650 – 700°C at SHS conditions compared to SCW conditions. Therefore, while both UO<sub>2</sub> and MOX may be used as fuel in SHS channels, an alternative fuel with higher thermal conductivity should be used as fuel in SCW channels.

### 3. Conclusions

Heat-transfer calculations were performed for a SCW and a SHS channel. Four different AHFPs and two fuels were considered. Calculations were performed for average channel power for a generic SCWR. It was found that while UO<sub>2</sub> may be used as fuel in SHS channels, an alternative fuel with higher thermal conductivity should be used as fuel in SCW channels.

### Nomenclature

$c_p$	specific heat at constant pressure, J/kg·K
$D_{hy}$	hydraulic-equivalent diameter, m
$h$	specific enthalpy, kJ/kg
$k$	thermal conductivity, W/m·K
$m'$	mass flow-rate, kg/s
$q'$	linear heat flux, W/m
$P$	pressure, Pa
$T$	temperature, °C

### Greek symbols

$\mu$	dynamic viscosity, Pa·s
$\rho$	density, kg/m <sup>3</sup>

### Non-dimensional numbers

$Nu_b$	Nusselt Number
$Pr_b$	Prandtl Number
$Re_b$	Reynolds Number

### Subscripts

b	bulk-fluid
el	electrical
in	inlet
out	outlet
w	wall

## References

- [1] Duffey, R.B., Pioro, I., Zhou, T., Zirn, U., Kuran, S., Khartabil, H. and Naidin, M. "Supercritical Water-Cooled Nuclear Reactors (SCWRs): Current and Future Concepts - Steam-Cycle Options". Proc. ICONE-16, Orlando, Florida, USA, May 11-15, 2008, Paper #48869, 9 pages.
- [2] Pioro, I. L., & Duffey, R. "Heat Transfer and Hydraulic Resistance at Supercritical Pressure in Power-Engineering Applications". NY, USA: ASME Press, 2007.
- [3] Leung, L.K.H.. "Effect of CANDU Bundle-Geometry Variation on Dryout Power". Proc. ICONE-16, Orlando, Florida, USA, May 11-15, 2008, Paper #48827.
- [4] Allison, L., Villamere, B., Grande, L., Mikhael, S., Rodriguez- Prado, A. and Pioro, I., 2009. "Thermal Design Options for SCWR Fuel Channel with Uranium Carbide and Uranium Di- Carbide Ceramic Fuels". Proc. of ICONE17, July 12-16, Brussels, Belgium, Paper #75975, 10 pages.
- [5] Zahlan, H., Groeneveld, D. and Tavoularis, S., 2010. Look-Up Table for Trans-Critical Heat Transfer, Proc. 2nd Canada-China Joint Workshop on Supercritical Water-Cooled Reactors (CCSC-2010), Toronto, Ontario, Canada: Canadian Nuclear Society, April 25-28
- [6] Mokry, S., Gospodinov, Ye., Pioro, I. and Kirillov, P., 2009a. Supercritical Water Heat-Transfer Correlation for Vertical Bare Tubes, Proceedings of the 17th International Conference on Nuclear Engineering (ICONE-17), Brussels, Belgium, July 12-16, Paper#76010, 8 pages.
- [7] Sweet, J. N., Roth, E. P., & Moss, M.. "Thermal Conductivity of Inconel 718 and 304 Stainless Steel". *International Journal of Thermophysics*. Vol. 8, No. 5, 1987, 14 pages.